molecular pharmaceutics

articles

Thermodynamics of Lipophilic Drug Binding to Intestinal Fatty Acid Binding Protein and Permeation across Membranes

Tony Velkov*

Medicinal Chemistry and Drug Action, Monash Institute of Pharmaceutical Sciences, Monash University (Parkville Campus), 381 Royal Parade, Parkville, Victoria 3052, Australia

Received November 1, 2008; Revised Manuscript Received January 8, 2009; Accepted February 4, 2009

Abstract: Intestinal fatty acid binding protein (I-FABP) is present at high levels in the absorptive cells of the intestine (enterocytes), where it plays a role in the intracellular solubilization of fatty acids (FA). However, I-FABP has also been shown to bind to a range of non-FA ligands, including some lipophilic drug molecules. Thus, in addition to its central role in FA trafficking, I-FABP potentially serves as an important intracellular carrier of lipophilic drugs. In this study we provide a detailed thermodynamic analysis of the binding and stability properties of I-FABP in complex with a series of fibrate and fenamate drugs to provide an insight into the forces driving drug binding to I-FABP. Drug binding and selectivity for I-FABP are driven by the interplay of protein−ligand interactions and solvent processes. The Gibbs free energies ($\Delta G°$) determined from dissociation constants at 25 °C ranged from −6.2 to −10 kcal/mol. The reaction energetics indicate that drug binding to I-FABP is an enthalpy−entropy driven process. The relationship between I-FABP stability and drug binding affinity was examined by pulse proteolysis. There is a strong coupling between drug binding and I-FABP stability. The effect of an I-FABP protein sink on the kinetics and thermodynamics of tolfenamic acid permeation across an artificial phospholipid membrane were investigated. I-FABP significantly decreased the energy barrier for desorption of tolfenamic acid from the membrane into the acceptor compartment. Taken together, these data suggest that the formation of stable drug−I-FABP complexes is thermodynamically viable under conditions simulating the reactant concentrations likely observed *in vivo* and maybe a significant biochemical process that serves as a driving force for passive intestinal absorption of lipophilic drugs.

Keywords: Intestinal fatty acid binding protein; drug absorption; lipophilic drug binding; intracellular drug transport

Introduction

A major limiting factor in the development of clinically useful drugs is poor and variable drug absorption.[1,2] With few exceptions drug candidates that are not absorbed after oral administration fail during development due to the low patient acceptability of other routes of administration. The processes by which lipophilic drugs are transported across the hydrophilic environment of the cytosol of adsorptive cells of the small intestinal epithelia (enterocytes) is a key factor limiting the effective design of drug candidates with optimal absorption characteristics.[1,2] Knowledge of structure−transport relationships will allow for directed structural modifications of drug candidates aimed at circumventing these diffusional barriers.

* Mailing address: Monash Institute of Pharmaceutical Sciences, Medicinal Chemistry and Drug Action, 381 Royal Parade, Parkville, Melbourne, Victoria 3052, Australia. Phone: +61-3-99039539. Fax: +61-3-99039582. E-mail: Tony.Velkov@pharm.monash.edu.au.

(1) Martinex, M. N.; Amidon, G. L. A mechanistic approach to understanding the factors affecting drug absorption: A review of fundamentals. *J. Clin. Pharmacol.* **2002**, *42*, 620–643.

(2) Sun, D.; Yu, L. X.; Hussain, M. A.; Wall, D. A.; Smith, R. L.; Amidon, G. L. In vitro testing of drug absorption for drug "developability" assessment: forming an interface between in vitro preclinical data and clinical outcome. *Curr. Opin. Drug Discovery Dev.* **2004**, *7*, 75–85.

10.1021/mp800227w CCC: $40.75
Published on Web 03/06/2009

In a recent series of reports we have shown that the innate intestinal-type intracellular fatty acid binding protein (I-FABP) potentially facilitates the absorption of orally administered lipophilic drug compounds.[3,4] I-FABP was shown to bind a diverse set of lipophilic drugs and enhance their permeability across an artificial membrane intestinal permeability model.[3,4] FABPs are a subclass of the intracellular lipid binding protein (iLBPs) family that constitutes a diverse group of low molecular weight (12−15 kDa) intracellular polypeptides.[5−7] Although the precise intracellular function of FABPs remains unclear, they have been implicated in the intracellular solubilization and transport of FA.[5−7] FABPs appear to act as intracellular shuttles for FAs to the nucleus, where the FA is released to nuclear receptors such as peroxisome proliferator activated receptors (PPARs) thereby effecting transcriptional regulation of metabolic enzymes and transporters that target the activating ligand.[8−11] In absorptive tissues such as the intestine, the FABP-PPAR signaling pathway functions to reduce absorption and exposure to the rest of the body. Hypolipidemic fibrate-type drugs are known to operate via the PPAR nuclear receptor agonist pathway, stimulating the upregulation of lipid metabolizing enzymes and transporters such as FABPs.[8−11] Our understanding of how drug binding events to specific nuclear receptors produce a biological response on the activating drug is mostly limited to the transcriptional events in the nucleus, whereas mechanisms of selective accumulation and intracellular transport to specific targets remain largely unknown.

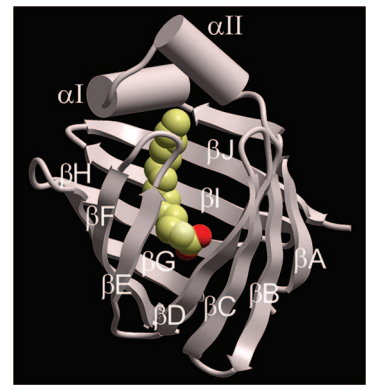

Figure 1. Schematic ribbon diagram of the crystallographic structure of I-FABP bound to myristate (PDB code: 1ICM). The secondary structure topology is indicated.

Although FABPs show a ubiquitous tissue and cellular distribution, their physiological functions are most pronounced in tissues highly active in lipid absorption and metabolism, such as the enterocyte cells lining the intestinal epithelia. In enterocytes, liver type (L)-FABP is coexpressed with the innate I-FABP, constituting as much as 3−6% of the cytosolic protein.[12,13] The relative intracellular concentrations of FABPs and FA indicate that significant quantities of apo-protein are present. This presents the possibility that FABPs also bind and facilitate the intracellular trafficking of exogenous lipophilic small molecules such as certain orally administered drugs.

FABPs possess similar tertiary structures, and are composed of ten antiparallel β-strands, which form a clamshell-like barrel structure (Figure 1). The interior of the β-barrel forms a large solvated ligand binding cavity, lined with a mixture of hydrophobic and polar/charged residues.[14] The β-barrel is capped by a pair of α-helices that modulate the cavity size and hydrophobicity to accommodate ligand entry.[14,15] A mechanism for ligand binding termed the "portal

(3) Velkov, T.; Chuang, S.; Wielens, J.; Sakellaris, H.; Charman, W. N.; Porter, C. J.; Scanlon, M. J. The Interaction of Lipophilic Drugs with Intestinal Fatty Acid-binding Protein. *J. Biol. Chem.* **2005**, *280*, 17769–17776.
(4) Velkov, T.; Horne, J.; Laguerre, A.; Jones, E.; Scanlon, M. J.; Porter, C. J. Examination of the role of intestinal fatty acid-binding protein in drug absorption using a parallel artificial membrane permeability assay. *Chem. Biol.* **2007**, *14*, 453–465.
(5) Banaszak, L.; Winter, N.; Xu, Z.; Bernlohr, D. A.; Cowan, S.; Jones, T. A. Lipid-binding proteins: a family of fatty acid and retinoid transport proteins. *Adv. Protein Chem.* **1994**, *45*, 89–151.
(6) Coe, N. R.; Bernlohr, D. A. Physiological properties and functions of intracellular fatty acid-binding proteins. *Biochim. Biophys. Acta* **1998**, *1391*, 287–306.
(7) Lucke, C.; Gutie'rrez-Gonza'lez, L. H.; Hamilton, J. Intracellular lipid binding proteins: evolution, structure and ligand binding. In *Cellular Proteins and their Fatty Acids in Health and Disease*; Duttaroy, A. K., Spener, F., Eds.; Wiley-VCH: Weinheim, Germany, 2003.
(8) Wolfrum, C.; Borrmann, C. M.; Borchers, T.; Spener, F. Fatty acids and hypolipidemic drugs regulate peroxisome proliferator-activated receptors α- and γ-mediated gene expression via liver fatty acid binding protein: a signaling path to the nucleus. *Proc. Natl. Acad. Sci. U.S.A.* **2001**, *98*, 2323–2328.
(9) Helledie, T.; Antonius, M.; Sorenseb, R. V.; Hertzel, A. V.; Bernlohr, D. A.; Kolvraa, S.; Kristiansen, K.; Mandrup, S. Lipid-binding proteins modulate ligand-dependent *trans*-activation by peroxisome proliferator-activated receptors and localize to the nucleus as well as the cytoplasm. *J. Lipid Res.* **2000**, *41*, 1740–1751.
(10) Huang, H. O.; Starodub, A.; McIntosh, B. P.; Atshaves, G.; Woldegiorgis, A. B.; Kier, F.; Schroeder, F. Liver fatty acid-binding protein colocalizes with peroxisome proliferator activated receptor alpha and enhances ligand distribution to nuclei of living cells. *Biochemistry* **2004**, *43*, 2484–2500.
(11) Adida, A.; Spener, F. Intracellular lipid binding proteins and nuclear receptors involved in branched-chain fatty acid signaling. *Prostaglandins, Leukotrienes Essent. Fatty Acids* **2002**, *2−3*, 91–98.
(12) Paulussen, R. J.; Van Moerkerk, H. T.; Veerkamp, J. H. Immunochemical quantitation of fatty acid-binding proteins. Tissue distribution of liver and heart FABP types in human and porcine tissues. *Int. J. Biochem.* **1990**, *22*, 393–398.
(13) Bass, N. M.; Manning, J. A. Tissue expression of three structurally different fatty acid binding proteins from rat heart muscle, liver, and intestine. *Biochem. Biophys. Res. Commun.* **1986**, *137*, 929–935.
(14) Sacchettini, J. C.; Gordon, J. I. Rat intestinal fatty acid binding protein. A model system for analyzing the forces that can bind fatty acids to proteins. *J. Biol. Chem.* **1993**, *268*, 18399–18402.
(15) Hodsdon, M. E.; Cistola, D. Discrete backbone disorder in the nuclear magnetic resonance structure of apo intestinal fatty acid-binding protein: implications for the mechanism of ligand entry. *Biochemistry.* **1997**, *36*, 1450–1460.

hypothesis" has been proposed, where the ligand enters the protein through a dynamic area formed by the helical region, before binding inside the cavity.[15] In the case of I-FABP the helical region has also been shown to serve an important role in collision-induced FA transfer events between I-FABP and membranes.[16] Although the precise mechanism of ligand entry remains unclear, kinetic binding studies with portal mutants have indicated that the initial ligand binding event possibly involves an interaction between the carboxyl moiety of the FA and a conserved arginine residue situated near the portal entrance.[17] Additionally, hydrophobic interactions between the FA methylene tail and nonpolar side chains on the protein's surface and portal region appear to be involved in the initial protein−ligand binding event.[18] These initial surface interactions are followed by internalization of the FA into the cavity where a more stable complex is formed. This unorthodox ligand recognition mechanism may also explain the apparent ligand promiscuity of the FA binding cavity. In theory, any lipophilic ligand that displays chemical properties that resemble a FA is a potential ligand for I-FABP. This is coincident with the high to moderate binding affinity interactions documented for I-FABP and carboxyl containing drugs with extended lipophilic tail components.[4]

The study of processes by which lipophilic drugs are transported across the enterocytic cytoplasm has been almost entirely neglected in the field of drug absorption. I-FABP is the ideal model iLBP for study due to its high abundance in the epithelium of the small intestinal tract where oral drug absorption predominately occurs. The need for an improved understanding of how lipophilic drugs are capable of binding to intracellular FA transporters such as I-FABP under physiological conditions has prompted this investigation into the thermodynamic properties of I-FABP in complex with a set of fibrate and fenamate drugs. We report on the thermodynamic driving forces responsible for drug binding to I-FABP as available from van't Hoff enthalpies. The data are discussed in relation to the binding mode of each drug as determined by NMR.[4] The stability of each drug−I-FABP complex were examined by the pulse proteolysis denaturant unfolding method. Furthermore, the influence of I-FABP on the kinetics and thermodynamics of drug permeation across artificial phospholipid membranes is examined. The potential role of I-FABP in facilitating passive drug absorption is discussed based on correlations established between the macroscopic thermodynamic quantities and microscopic changes at the molecular level. In particular the data presented signal a step change in our understanding of the way in which lipophilic drug molecules transverse the apical membrane barrier of the enterocyte.

Materials and Methods

Materials. Isopropyl β-D-thiogalactopyranoside (IPTG) was purchased from BioVectra (Prince Edward Island, Canada). Drug compounds were obtained from Sigma-Aldrich (Sydney, NSW, Australia). *Escherichia coli* strain BL21 Codon Plus (DE3)-RIL was purchased from Stratagene (La Jolla, CA). All other reagents were of the highest purity commercially available.

Expression and Purification of Rat I-FABP. The cDNA of rat I-FABP (FABP2) was isolated and ligated into the pTrc99 expression vector and expressed under control of *lacI*^{q} gene, with IPTG induction. The pTrc99-rat-I-FABP expression plasmid is available from the Addgene Plasmid Repository (http://addgene.org) under the plasmid identification code 13578. Protein expression was induced by the addition of 1 mM IPTG to liquid cultures at a cell density of $OD_{600nm} = 0.6$. The recombinant protein was expressed for 6 h and purified from *E. coli* BL21 Codon Plus (DE3)-RIL cells as described previously.[3] ^{15}N labeled protein for NMR experiments was produced by over-expression in M9 minimal media containing $^{15}NH_4Cl$. Typical yields of protein following purification and delipidation were 10−15 mg per liter of culture for minimal media cultures and 15−25 mg for unlabeled expressions in Luria−Bertani media. The homogeneity of the purified protein was ascertained to be ≥98% by SDS−PAGE/silver staining and electrospray ionization mass spectrometry (Supplementary Figure 1 in the Supporting Information).

NMR ^{1}HN−^{15}N Backbone Amide Chemical Shift Mapping. For drug titration experiments, 600 μL samples of 50 μM ^{15}N-I-FABP were prepared in 90% H_2O/10% D_2O in 20 mM MES, pH 5.5; 50 mM NaCl buffer. Drugs were titrated into the protein solution to final concentrations of 0−2.0 mM from a DMSO stock solution, the final DMSO level were <2% (v/v). 2D ^{1}H−^{15}N heteronuclear single quantum coherence (HSQC) spectra were acquired on a Varian ANOVA 600 MHz spectrometer operating at 25 °C. Spectra were processed with the software package NMRPipe[19] and assigned using the program SPARKY.[20] The combined ^{1}HN and ^{15}N backbone amide nuclei chemical-shift changes ($\Delta\delta_{comb}$) between apo- and holo-I-FABP assignments were calculated using the square root of the sum of the weighted squares of the ^{1}HN and ^{15}N backbone amide chemical shift values (eq 1),

$$\Delta\delta_{comb} = \sqrt{(\omega_{HN}\Delta\delta^1H)^2 + (\omega_N\Delta\delta^{15}N)^2} \qquad (1)$$

where $\Delta\delta^1$HN and $\Delta\delta^{15}$N denote the ^{1}HN and ^{15}N backbone amide chemical shift change between the apo- and holo-

(16) Storch, J.; Herr, F. M.; Hsu, K. T.; Kim, H. K.; Liou, H.; Smith, E. R. The role of membranes and intracellular binding proteins in cytosolic transport of hydrophobic molecules: Fatty-acid binding proteins. *Comp. Biochem. Physiol.* **1996**, *15B*, 333–339.

(17) Richieri, G. V.; Low, P. J.; Ogata, R. T.; Kleinfeld, A. M. Binding Kinetics of Engineered Mutants Provide Insight about the Pathway Entering and Exiting the Intestinal Fatty Acid Binding Protein. *Biochemistry* **1999**, *38*, 5888–5895.

(18) Friedman, R.; Nachliel, E.; Gutman, M. Fatty Acid Binding Proteins: Same Structure but Different Binding Mechanisms Molecular Dynamics Simulations of Intestinal Fatty Acid Binding Protein. *Biophys. J.* **2006**, *90*, 1535–1545.

(19) Delaglio, F.; Grzesiek, S.; Vuister, G. W.; Zhu, G.; Pfeifer, J.; Bax, A. NMRPipe: a multidimensional spectral processing system based on UNIX pipes. *J. Biomol. NMR* **1995**, *6*, 277–293.

(20) Goddard, T. D., and Kneller, D. G. (2006). SPARKY 3 (http://www.cgl.ucsf.edu/home/sparky).

protein for a particular residue and ω_i denotes the weight factor of the nucleus which accounts for differences in sensitivity of the ^{1}HN and ^{15}N, $\omega_H = 1.0$, $\omega_N = 0.154$. Weight factors are determined from the ratio of the average standard deviations of the chemical shifts for a given nucleus type observed for the 20 proteogenic amino acids using the BioMagResBank chemical shift database. The $\Delta\delta_{comb}$ were normalized to the maximum $\Delta\delta_{comb}$ for the particular data set. Residues that displayed chemical shift perturbations were mapped onto the crystallographic structure of rat I-FABP in complex with palmitic acid (PDB code: 2IFB) to visualize the movement of backbone amides. Molecular visualization was performed using the software packages PYMOL (Delano Scientific, San Carlos, CA).

Pulse Proteolysis of Drug−I-FABP Complexes in Urea. Pulse proteolysis of drug−I-FABP complexes was performed as previously described with minor modifications to the protocol.[21] To monitor I-FABP stability in the presence of drug, the protein was equilibrated with the ligand for 1 h at 25 °C, before the addition of urea to the reaction mixture. Reaction mixtures consisted of I-FABP (30 μM) with 0.5 mM ligand in 20 mM Tris-HCl pH 8.0, 50 mM NaCl, 10 mM $CaCl_2$ and urea to a final concentration of 0−8 M. To establish equilibrium between the folded and the unfolded state, reaction mixtures in urea were incubated for 24 h prior to proteolysis. Proteolyis was initiated by the addition of thermolysin to a final concentration of 0.2 mg/mL, and the mixture was incubated at 25 °C for 1 min. Proteolysis was quenched by the addition of 3 mM EDTA (pH 8) and the addition of one volume of SDS−PAGE sample buffer (12.5% 0.5 M Tris-HCl pH 6.8; 0.005% bromophenol blue; 10% SDS; 10% glycerol; 2% β-mercaptoethanol) and heated for 2 min at 100 °C. Samples were resolved on 4% stacking, 15% resolving polyacrylamide gels at 4 °C at a constant voltage of 80 V, using the Laemmli buffer system.[22] Gels were stained with Coomassie Blue G-250, and destained with 50% methanol/10% acetic acid (v/v) solution. Gels were dried between cellulose sheets and scanned at 1200 dpi. Protein bands were quantified densitometrically using OneD-scan 1D gel analysis software V2.03 (Scanalytics).

The fraction of folded protein ($F_{fold} = I/I_0$) was determined from the intensity of the I-FABP protein band in the presence of urea (I) divided by the band intensity of I-FABP in the absence of urea (I_0). The denaturant concentration at which half of the protein is unfolded (C_m) and the m value ($m = \Delta G_{unf}^\circ/[\text{denaturant}]_{1/2}$, representing the denaturant dependence of ΔG_{unf}°), were determined by fitting F_{fold} to eq 2,[21]

$$F_{fold} = F_0(1/1 + \exp(-\Delta G_{unf}^\circ/RT)) \quad (2)$$

where F_0 represents the fraction of folded protein in the absence of urea ($F_0 = 1.0$); The global stability of the protein is $\Delta G_{unf}^\circ = -m(C_m - [\text{urea}])$; R is the gas constant (1.99 cal/(mol K)); T is the reaction temperature (25 °C) in kelvins (298.15 K). Because m values determined by pulse proteolysis are not entirely reliable for the calculation of ΔG_{unf}° (due to insufficient data in the transition zone),[21] an m value for I-FABP was estimated using a statistical method that estimates m values from the molecular size of the protein.[23] For urea denaturation the m value is estimated by multiplying the number of residues in the protein by a value of −0.013 kcal mol^{-1}; the m value of I-FABP (131 residues) was estimated to be −1.7 kcal/(mol.M). ΔG_{unf}°, the Gibbs free energy of global unfolding, which represents the difference in stability between the unfolded and native state, was calculated from $\Delta G_{unf}^\circ = -mC_m$.

To ensure that proteolysis of the folded protein during the 1 min pulse is negligible, a control experiment was performed where the protein is digested near the C_m and the proteolytic rate is measured. Proteolysis of I-FABP in 3.5 M urea was monitored for 10 min. Changes in the intensity of the 15 kDa I-FABP band corresponding to the intact protein were plotted as a function of time and fitted to a first-order rate equation to determine the observed proteolytic rate constant (k_{obs}):

$$I/I_0 = (I_0 - I)\exp(-k_{obs}t) + I \quad (3)$$

where I is the band intensity at a cleavage time; I_0 is the band intensity at $t = 0$; t is the time in minutes.

Fluorometric Binding Affinity Measurements for the Determination of Van't Hoff Enthalpies. Drug binding affinity was measured fluorometrically by monitoring the displacement of the fluorescent binding cavity probe 1-anilino-8-naphthalene sulfonic acid (ANS) as previously described.[3] Briefly, fluorometric measurements were performed under steady-state conditions on a Cary Eclipse fluorescence spectrophotometer (Varian, Mulgrave, Victoria, Australia) in 20 mM Tris-HCl, pH 8.0; 50 mM NaCl buffer. The decrease in ANS fluorescence upon addition of competing ligand was monitored and plotted as a function of the concentration of competing ligand. The data were fitted by nonlinear regression to a one-site competition model from which EC_{50} values were derived. The inhibition constant (K_i) for ligand binding were calculated according to eq 4:

$$K_i = EC_{50}/(1 + [\text{ANS}]/K_{d\,ANS}) \quad (4)$$

K_i values for each drug−I-FABP interaction were determined at several different temperatures and a van't Hoff plot (eq 5) of $\ln(K_d)$ versus $1/T$ (which is a straight line if the heat capacity is independent of temperature), from which ΔH° is determined from the slope.

The non-integrated linear form ($y = a + bx$) of the van't Hoff equation is

(21) Park, C.; Marqusee, S. Pulse proteolysis: A facile method for quantitative determination of protein stability and ligand binding. *Nat. Methods* **2005**, *2*, 207–212.

(22) Laemmli, U. K. Cleavage of structural proteins during the assembly of the head of bacteriophage T4. *Nature* **1970**, *227*, 680–685.

(23) Myers, J. K.; Pace, C. N.; Scholtz, J. M. Changes in accessible surface areas of protein unfolding Denaturant m values and heat capacity changes. *Protein Sci.* **1995**, *4*, 2138–2148.

$$\ln(K_d) = (\Delta H°/RT) - \Delta S°/R \quad (5)$$

A plot of $y = \ln(K_d)$ versus $x = 1/T$ yields a straight line with a slope $b = \Delta H°/R$ and a y-intercept, $a = -\Delta S°/R$, where R is the universal gas constant, 1.99 cal/(mol K).

The Gibbs free energy change ($\Delta G°$) for each drug−I-FABP binding reaction was calculated from the equilibrium dissociation constant at 25 °C as $\Delta G° = -RT \ln(K_d)$. Entropies ($-T\Delta S°$) were determined using $\Delta G° - \Delta H°$.

Bio- and Chemi-informatics Methods. The chemical properties of the test compounds were calculated using Chem3D v10.0 (Cambridge Soft) and Advance Chemistry Development software v6.0 (ACD Laboratories, Toronto, Canada). Interatomic protein−ligand contacts were analyzed using the automated LPC/CSU server.[24]

Parallel Artificial Membrane Permeability Assay (PAMPA). The effect of an I-FABP protein sink on the kinetics and thermodynamics of permeation of tolfenamic acid through phospholipid membranes was investigated in the PAMPA (*p*ION, Woburn, MA) *in vitro* intestinal permeability system. PAMPA consists of a "sandwich" assembly formed from a 96-well microfilter acceptor plate (Millipore Multiscreen, Sydney, NSW, Australia) and an indented 96-well donor plate (*p*ION, Woburn, MA). Each composite well of the assembly is divided into two chambers, a donor at the bottom and acceptor at the top separated by a 125 μm thick hydrophobic polyvinylidene fluoride (PVDF) microfilter disk (0.45 μm pore size). The disk of each well is coated with a 2% (w/v) dodecane solution of 1,2-dioleoyl-*sn*-glycero-3-phosphocholine (*p*ION P/N 110669) that forms multilamellar lipid bilayers inside the filter channels when in contact with an aqueous buffer solution. The donor and acceptor solutions contained an identical buffer composition (20 mM Tris pH 7.4; 50 mM NaCl). The donor buffer solutions contained 2.5 mM tolfenamic acid (including <1% (v/v) DMSO); an excess of compound is present in the donor compartment to ensure that the donor solution is maintained at a constant drug concentration and does not become limiting during the course of the experiment. Membranes were saturated with drug donor solution for 2 h at the studied temperatures before carrying out the permeation studies. Acceptor solutions contained buffer or 0.33 mM I-FABP. The acceptor filter plate was placed on top of the donor plate forming the "sandwich" and incubated for 0.5−7.0 h. PAMPA measurements were carried out at temperatures of 10−37 °C. At the appropriate sampling points, the PAMPA sandwich was separated and the tolfenamic acid concentration in both donor and acceptor compartments was assayed by UV−vis spectrophotometry from the peak absorbance at 286 nm.

The permeability coefficient (disappearance P_e) describing solute uptake into the membrane; the permeability coefficient describing donor-to-acceptor transmembrane transport (appearance P_e) and the proportion of material retained in the phospholipid membrane barrier (% R) were calculated as previously described in detail.[4] For both uptake into the membrane and transport across the membrane from the donor to acceptor, P_e is an effective membrane permeability coefficient and reflects the composite drug permeability across both the hydrodynamic diffusion layers and the membrane. All experiments were performed in triplicate and data are reported as mean ± standard deviation.

The membrane permeation of a drug requires energy to facilitate the mass transfer of the drug molecules across the membrane and hydrodynamic layers. The temperature dependence of the permeability coefficient is linked to the energy activated processes of solvation and diffusion of the drug. Accordingly, the permeability coefficient increases with temperature according to the Arrhenius relationship[25] (eq 6):

$$\log P_e = \log A - [\Delta Ep + \Delta Hp/2.303RT] \quad (6)$$

$\Delta Ep + \Delta Hp$ is the total activation energy required for permeation and equals the sum of the activation energy for membrane diffusion (ΔEp) and the energy required for solvation of the drug in the media (ΔHp). A is an empirical constant called the frequency factor which includes the frequency of collisions and their orientation. R is the universal gas constant, and T the temperature in kelvins. The total activation energy required for membrane permeation can be determined experimentally by measuring the rate of drug permeation at various temperatures. Then according to the Arrhenius relationship a plot of $\ln P_e$ versus the reciprocal of the absolute temperature in kelvins yields a straight line, the slope of which equals $-(\Delta Ep + \Delta Hp)/R$ and a y-intercept of $\ln A$.

Results

Denaturant Stability of Drug−I-FABP Complexes Measured by Pulse Proteolysis. The test compounds absorb strongly in the wavelength regions used to monitor protein unfolding by UV−vis and fluorescence spectroscopy; therefore measurements of the effect of these compounds on the denaturant stability of I-FABP are not possible using these spectroscopic detection methods. Pulse proteolysis is a method of considerable utility for examining the effect of ligands on protein stability when the ligand is not compatible with other spectroscopic methods. Pulse proteolysis is designed to digest only target protein molecules that are unfolded. The time of the proteolyic pulse (1 min) is much shorter than the relaxation time between the folded and unfolded proteins in the equilibrium mixture, thus only the unfolded protein molecules are digested. Because excess protease is present in the equilibrium mixture, digestion of the unfolded proteins occurs rapidly with the rate constant of intrinsic proteolysis of the exposed proteolyic sites,

(24) Sobolev, V.; Sorokine, A.; Prilusky, J.; Abola, E. E.; Edelman, M. Automated analysis of interatomic contacts in proteins. *Bioinformatics* **1999**, *15*, 327–332.

(25) Ghannam, M. M.; Tojo, K.; Chien, Y. M. Kinetic and thermodynamics of drug permeation through silicone elastomers (I) Effect of penetrant hydrophilicity. *Drug Dev. Ind. Pharm.* **1986**, *12*, 303–325.

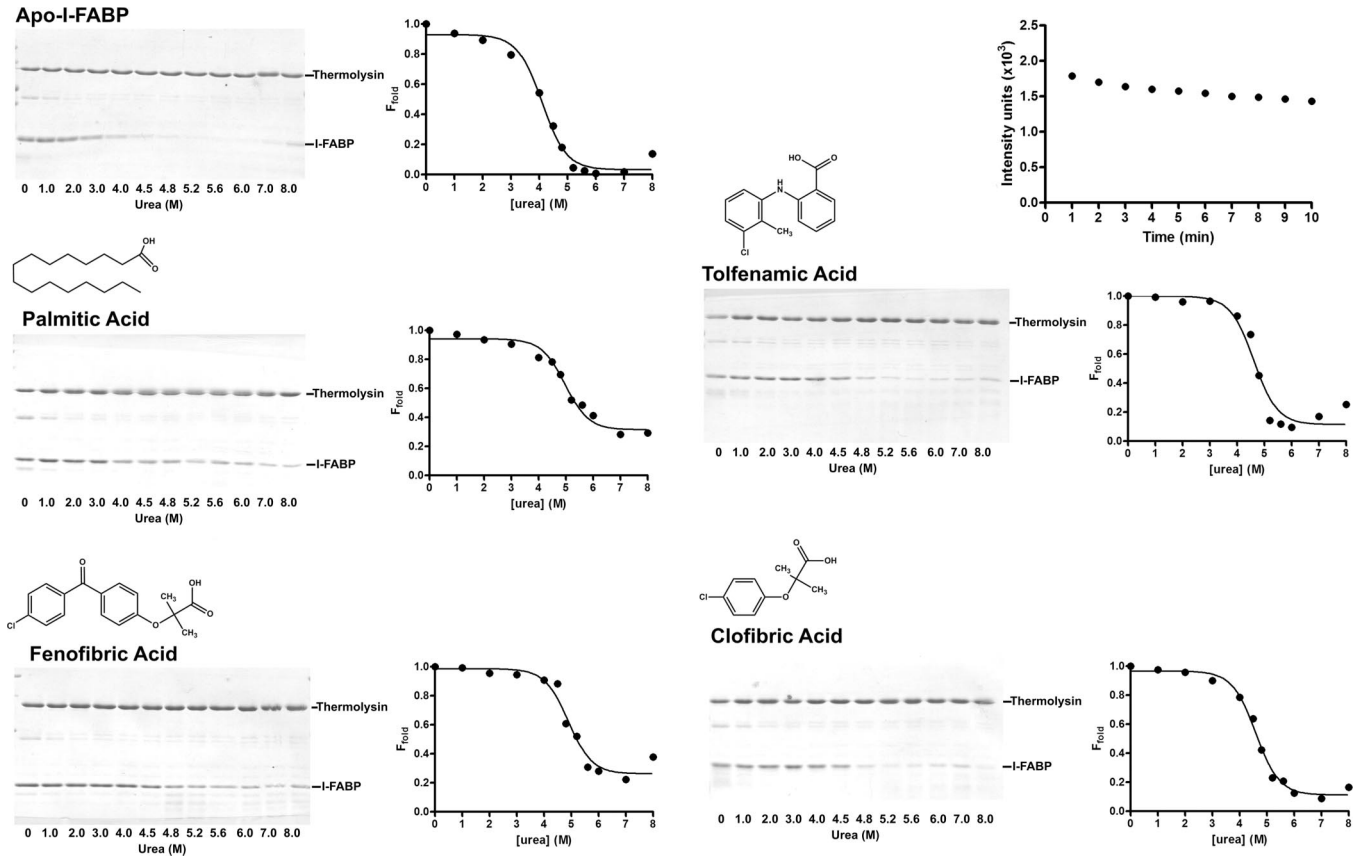

Figure 2. Global stability of I-FABP in complex with drugs measured by pulse proteolysis. Left panels: SDS−PAGE gel profiles of 1 min proteolytic pulse reactions of apo- and holo-drug−I-FABP complexes in the presence of increasing concentrations of urea. The protein band corresponding to intact I-FABP and the protease thermolysin are indicated. The intensity of the I-FABP band was quantified desitometrically and used to calculate the fraction of folded protein (F_{fold}). Right panels: F_{fold} plotted as a function of the urea concentration. The solid line represents the nonlinear least-squares fit of F_{fold} to eq 2 from which C_m values were determined. Top right panel: Proteolysis of I-FABP in 3.5 M urea was followed for 10 min. The band intensity was plotted as a function of digestion time.

whereas proteolysis of the folded species is slow and negligible within the time frame of the pulse. In line with the original protocol, thermolysin was found to be the most suitable proteolytic enzyme for this assay due to its broad specificity and ability to function in the presence of high concentrations of urea, thereby ensuring complete digestion of unfolded protein at most concentrations of denaturant. An important criterion for the success of this assay is that the folded protein is not significantly digested within the pulse period; this can occur if intrinsically unstructured regions are present in the native structure. Although I-FABP displays intrinsically unstructured regions within the portal,[15] there was no apparent digestion in the absence of denaturant within the 1 min pulse period employed for these experiments. As a further precaution control experiments were performed where proteolysis was monitored near the transition zone (3.5 M urea) for 10 min (Figure 2). The results show that the extended pulse period did not result in significant digestion of folded protein in the equilibrium mixture. Thus in the presence of urea, folded I-FABP in the equilibrium mixture should remain intact within the 1 min pulse, providing a reliable estimate of the fraction of folded protein (F_{fold}). The amount of folded protein that remained after the 1 min proteolytic pulse was determined by densitometric quantification of SDS−PAGE protein bands, and was used to calculate F_{fold} (Figure 2). As the urea concentration is increased, the two-state equilibrium is shifted toward the unfolded, proteolytically susceptible form. In the apo-form I-FABP remained resistant to proteolysis at urea concentrations up to 2 M, and rapidly decreased in the 3−5 M concentration range, and completely disappeared at 6−7 M urea, consistent with the cooperative transition of protein unfolding. At the highest urea concentration (8 M), some folded I-FABP remained, which can be attributed to the reduced catalytic activity of thermolysin at very high concentrations of denaturant. The denaturant concentration at which F_{fold} is 0.5 (C_m) was determined by fitting F_{fold} as a function of the urea concentration to a two state equilibrium unfolding model (Figure 2). The midpoint of transition (C_m) is a function of the stability and the m value of the protein. Therefore, the global stability of the protein (ΔG_{unf}°) was calculated by multiplying the C_m value determined from pulse proteolysis by the estimated m value for I-FABP. Table 1 documents the stability parameters determined by pulse proteolysis for apo- and the holo-drug−I-FABP complexes.

Table 1. Stability of Drug−I-FABP Complexes Determined by Pulse Proteolysis Urea Unfolding Measurements

drug	C_m[a] (M)	$\Delta G_{unf}°$ (kcal/mol)	$\Delta\Delta G_{unf}°$ (kcal/mol)
apo-I-FABP	4.1	7.0	na[b]
palmitic acid	5.0	8.5	1.5
fenofibric acid	4.9	8.3	1.3
tolfenamic acid	4.7	8.0	1.0
clofibric acid	4.5	7.7	0.7

[a] Concentration of urea at which half of the protein is unfolded. [b] Not applicable.

The $\Delta G_{unf}°$ values obtained for the apo-protein by this method were in agreement with those reported for equilibrium urea unfolding detected by spectroscopic methods.[26] Table 1 also lists the calculated change in the global stability ($\Delta\Delta G_{unf}°$) in the presence of ligand relative to the apo-protein. The C_m and $\Delta G_{unf}°$ values increased significantly in the presence of each drug. Drug binding to I-FABP contributes significantly (0.7−1.5 kcal/mol) to the global stability of the protein at the physiologically relevant drug concentrations tested. The bound drug stabilizes the folded conformation of the protein by slowing its unfolding, observed as an increased resistance to proteolysis. The high affinity compounds palmitic acid and fenofibric acid stabilized I-FABP so significantly that even high urea concentrations cannot completely unfold the protein. Both stability parameters displayed a dependence on the ligand binding affinity, with the order of decreasing C_m and $\Delta G_{unf}°$ values: palmitic acid > fenofibric acid > tolfenamic acid > clofibric acid. It is evident from the increase in C_m values and the apparent decrease in unfolding rate that drug binding affects both the stability and kinetics of unfolding of the I-FABP structure. In a control experiment we tested for the possibility that the increase in folded I-FABP observed in the presence of ligands was due to an inhibition of thermolysin activity by each drug. The digestion of a test protein that does not bind these drugs, lac repressor, was examined. There was no inhibition of thermolysin activity evident in the presence of each test compound at the same concentrations used in the pulse proteolysis assays (data not shown).

Conformational Changes in the Backbone of I-FABP Induced upon Drug Binding Monitored by ^{1}H and ^{15}N Backbone Amide Chemical Shift Mapping. ^{1}HN and ^{15}N backbone amide chemical shift changes associated with ligand binding are related to the change of the dihedral ϕ, ψ-backbone angles, side chain dihedral angles and hydrogen bonding. Thus, both local conformational and proximal changes induced by drug binding can be conveniently monitored by recording a series of ^{1}H−^{15}N-HSQC spectra of I-FABP in the presence of increasing concentrations of drug (Figure 3, bottom panels). Chemical shift perturbations occurred for a large number of residues, indicating that a slight global conformational rearrangement occurs upon drug binding. Mapping the chemical shift perturbations onto the crystallographic backbone structure of I-FABP indicated that the most significant perturbations were concentrated within the helicies forming the portal region and the βC-βD and βE-βF sheets (Figure 3 top right panels; *cf.* Figure 1 for topological descriptors). The ligands with the higher affinity constants, palmitic acid and fenofibric acid, produced significantly greater perturbations within the portal region compared to the lower affinity compounds, tolfenamic and clofibric acid.

Tracking the titration of the binding cavity residue Phe^{93} provides some information on the chemical exchange regime of each drug−I-FABP complex on the NMR time scale (Figure 3, top left panels). Titrations with the high affinity compounds palmitic acid and fenofibric acid produced separate peaks for bound and free I-FABP. The chemical shift of the respective peaks remained the same; however, their relative intensity changed with varying ligand concentration due to signal broadening, reflecting the relative populations of bound versus free. This is characteristic of the complexes being in slow exchange on the NMR time scale. In comparison, titrations with the lower affinity compounds tolfenamic acid and clofibric acid produced peaks that displayed a progressive movement with each titration. This is consistent with a fast to intermediate exchanging complex on the NMR time scale.

Thermodynamics of Drug Binding to I-FABP: van't Hoff Enthalpies. Although there have been some reports in the literature of discrepancies between direct calorimetric enthalpies and indirect van't Hoff enthalpies,[27] it has been shown that both approaches yield the same values if the correct experimental setup and analysis are applied.[27] Van't Hoff enthalpies were determined from analysis of drug binding affinities measured at several temperatures (Supplementary Table 1 in the Supporting Information). Binding affinity measurements were performed using a fluorometric ANS displacement assay; ANS has previously been shown to bind competitively with FA within the ligand binding cavity of I-FABP.[3] The binding isotherms for each drug displayed a good fit to a model which describes a single class of independent binding sites.[3] Each compound displayed a binding stoichiometry (n) of 1 mol of drug/mol of protein. Figure 4A shows an overlay of the van't Hoff plots for each drug. The temperature dependence of the data for each compound does not deviate from linearity, indicating that changes in heat capacity over the temperature range are minimal and as such the van't Hoff enthalpy estimates from the slope of each linear regression line are valid. The corresponding van't Hoff thermodynamic parameters are reported in Table 2 and graphically represented in Figure 4B. In all cases, the binding interaction is exothermic, characterized by negative enthalpies. Apart from clofibric acid, the net free energy of binding for each compound was also associated with a moderate but favorable entropic contribution.

Impact of Drug−I-FABP Binding on the Energetics of Membrane Transport. To examine the hypothesis that drug binding to I-FABP in the cytosol energetically facilitates

(26) Ira, J.; Ropson, J. I.; Gordon, J.; Frieden, C. Folding of a Predominantly β-Structure Protein: Rat Intestinal Fatty Acid Binding Protein. *Biochemistry* **1990**, *29*, 9591–9599.

(27) Horn, J. R.; Russell, D.; Lewis, E. A.; Murphy, K. P. van't Hoff, and Calorimetric Enthalpies from Isothermal Titration Calorimetry: Are There Significant Discrepancies? *Biochemistry* **2001**, *40*, 1774–1778.

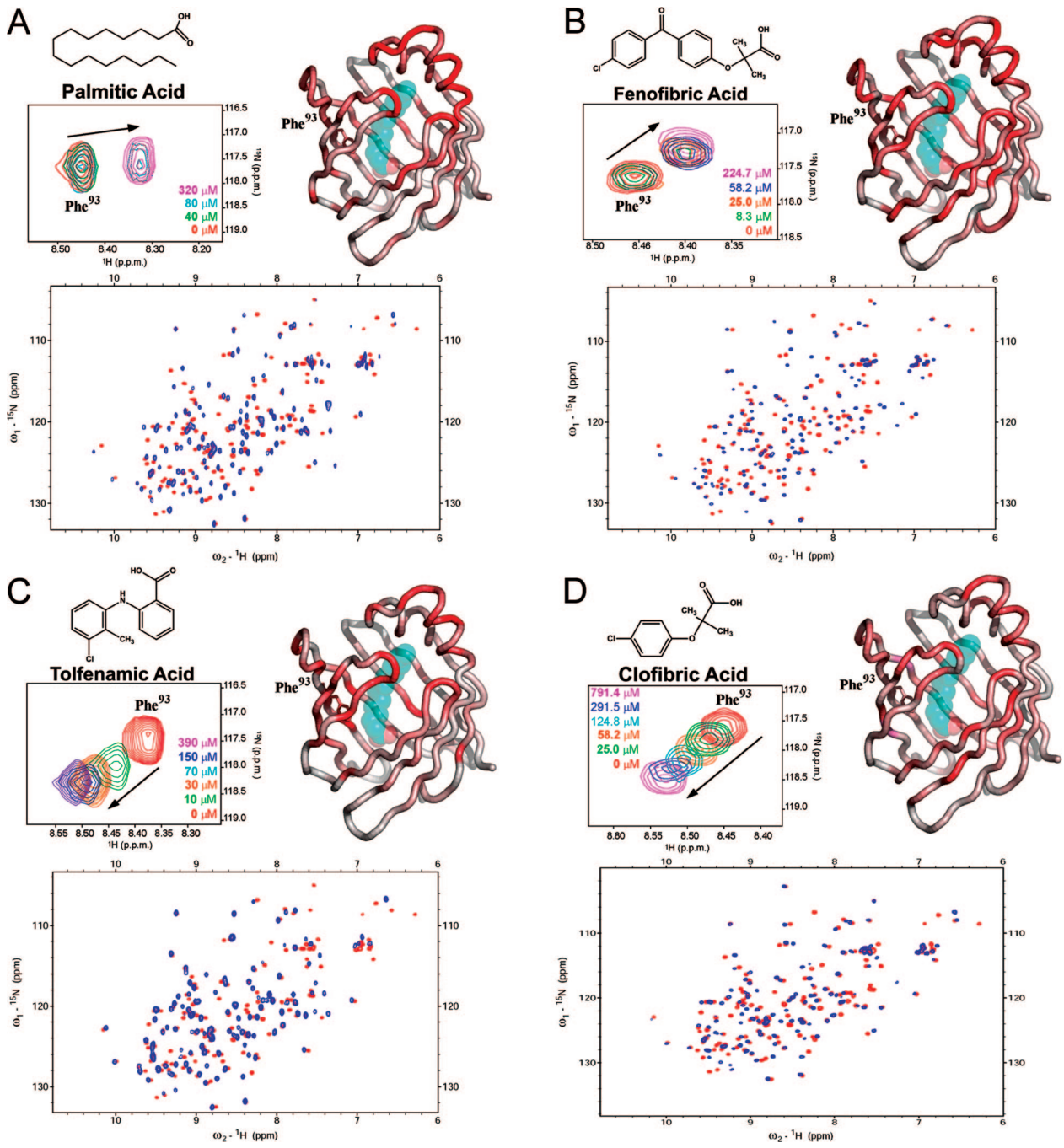

Figure 3. Backbone conformational changes in I-FABP induced by drug binding monitored by ^{1}HN and ^{15}N backbone amide chemical shift mapping. Top left: Magnified area showing the backbone ^{1}HN and ^{15}N chemical shifts perturbations of the binding cavity residue Phe^{93} upon titration of the I-FABP protein solution with a compound. The final concentration of drug in the sample at each titration point is indicated and colored to match the corresponding cross-peak. The direction of movement of the cross-peak in each titration is indicated by arrows. Top right: The ^{1}HN and ^{15}N chemical shift changes between the apo- and holo-drug bound states were mapped onto a tube representation the crystallographic backbone structure of rat I-FABP with bound palmitic acid shown in transparent sphere representation (2IFB). The intensity of the red color indicates the extent of the chemical shift perturbations between the apo- and holo-drug protein. The side chain of Phe^{93} is shown in stick representation. Bottom panel: Gradient- and sensitivity-enhanced ^{1}H/^{15}N HSQC spectrum for [U-99%-^{15}N] apo-I-FABP (red spectrum) and complexed with drug (blue spectrum) at 25 °C.

lipophilic drug transport across the apical absorptive membrane of the enterocyte and into the cytosol, a parallel artificial membrane permeability assay (PAMPA) has been utilized to model absorption events at the apical membrane domain (Figure 5D). Transport buffer was used in the donor chamber containing tolfenamic acid (simulating the small intestinal lumen), and the impact of either buffer or I-FABP (simulating the enterocytic cytosol) in the acceptor chamber

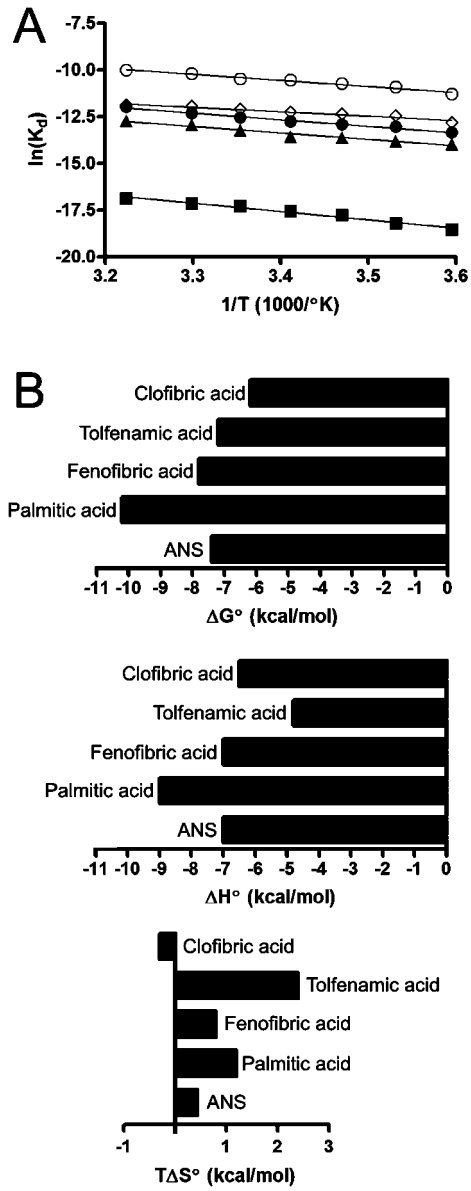

Figure 4. (A) van't Hoff plots for drug−I-FABP binding interactions: palmitic acid (■); fenofibric acid (▲); tolfenamic acid (◇); clofibric acid (○); ANS (●). The solid lines show a linear fit of the data sets; correlation coefficients ranged from 0.9483 to 0.9828 (1.0 indicating a perfect fit). Data points are the mean of three replicate experiments. (B) Dissection of the thermodynamic binding parameters. Binding enthalpies ($\Delta H°$) were obtained from the van't Hoff plots of the temperature dependence of K_d. The net free energy of binding ($\Delta G°$) were calculated from the K_d at 25 °C using $\Delta G° = RT \ln K_d$ and entropies ($-T\Delta S°$) were determined using $\Delta G° - \Delta H°$.

was evaluated. The concentration of I-FABP (0.33 mM) was chosen to reflect the cytosolic level of I-FABP reported in enterocytes.[12,13] The kinetics of permeation were measured at several temperatures. Under both acceptor chamber conditions, the rate of membrane permeation was found to increase with temperature, partly due to increased membrane fluidics. The presence of I-FABP in the acceptor chamber did not affect the kinetics of drug uptake into the membrane as observed from the rate of drug disappearance from the donor chamber (Figure 5A; Table 3). However, I-FABP significantly enhanced the rate of appearance of drug in the acceptor chamber (Figure 5A; Table 3). Importantly, the presence of I-FABP also reduced drug retention in the membrane and improved partitioning into the aqueous acceptor chamber (Figure 5B). An Arrhenius plot of the permeation rate as a function of the inverse of temperature yields a straight line the slope of which yields the activation energy for permeation (Figure 5C). The permeation rates appeared to converge at temperatures >28 °C due to the membrane phase transition, therefore these data points were omitted from the linear regression analysis. The activation energy of permeation for tolfenamic acid through the membrane was found to be 19.1 kcal/mol in the absence of an I-FABP sink and 13.7 kcal/mol with I-FABP in the acceptor chamber. Thus, the presence of a physiological concentration of I-FABP in the acceptor chamber markedly decreases (∼5.4 kcal/mol) the activation energy for membrane permeation of the lipophilic drug tolfenamic acid.

Table 2. van't Hoff Thermodynamic Parameters for Drug−I-FABP Complexes

drug	$\Delta G°$ (kcal/mol)	$\Delta H°$ (kcal/mol)	$T\Delta S°$ (kcal/mol)	drug $cLogD_{7.4}$[a]	drug $cSol_{7.4}$[a] (g/L)
ANS	−7.4	−7.0	0.44	−1.3	25
palmitic acid	−10	−9.0	1.2	4.5	0.91
fenofibric acid	−7.8	−7.0	0.8	−0.04	76
tolfenamic acid	−7.2	−4.8	2.4	2.3	2.6
clofibric acid	−6.2	−6.5	−0.3	−1.1	100

[a] Calculated log *D* and solubility at pH 7.4.

Discussion

This study is designed to provide a comprehensive thermodynamic and stability analysis of drug−I-FABP complexation in relation to the potential function of I-FABP in facilitating the process of drug absorption across the apical membrane of the enterocyte. The discussion is presented over a series of subheadings that cover the major conclusions that can be drawn from the biophysical data.

I-FABP Facilitates the Desorption of Lipophilic Drugs from Membranes. In order to be absorbed from the intestinal lumen, a drug must cross two diffusional barriers in series: the unstirred water layer and the apical membrane of the enterocyte. It is widely accepted that drug partitioning into the cell membrane is a rate determining step for passive membrane permeation.[28] For the absorption of relatively polar drug molecules, which have little intrinsic affinity for the lipophilic membrane, this is often the rate limiting process. In contrast, more lipophilic compounds normally partition readily into the cell membrane, but subsequently face the barrier of efficient transport across the hydrophilic environment of the cellular cytoplasm. I-FABP is among the most abundant proteins in the cytoplasm of the enterocyte

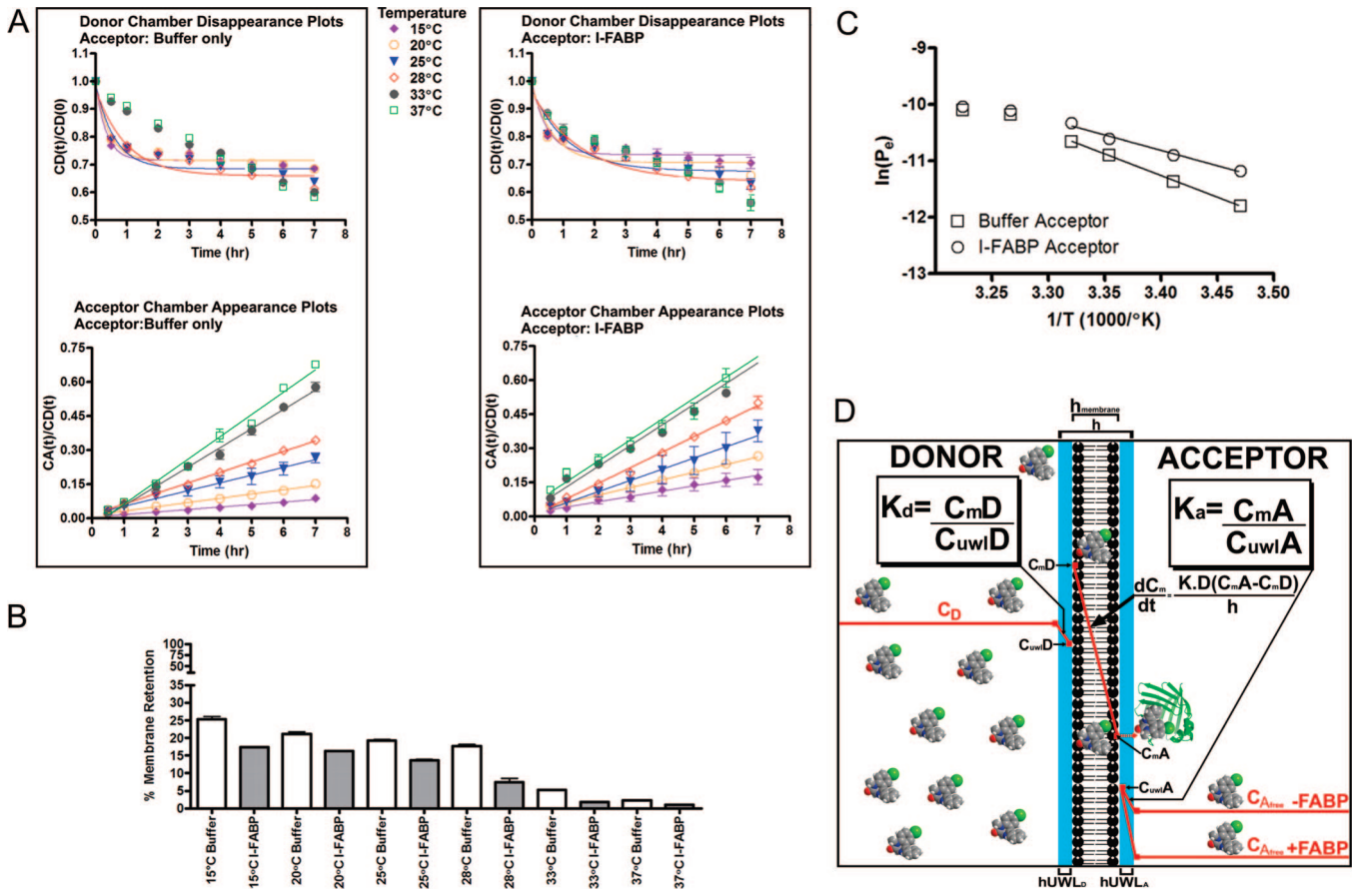

Figure 5. Impact of drug−FABP binding on energetics of membrane transport of tolfenamic acid. (A) The effect of temperature on the permeation rate of tolfenamic acid across a parallel artificial membrane permeability model. The kinetics for both the donor chamber (showing disappearance of drug versus permeation time) and acceptor chamber (showing appearance of drug versus permeation time) are shown for each temperature. Disappearance kinetics data are represented as the mass fraction in the donor chamber at time t [CD(t)] relative to time 0 [CD(0)]. Appearance kinetics data are represented as the mass fraction in the acceptor chamber [CA(t)] relative to the donor chamber [CD(t)] at time t. (B) The percentage of drug retained in the membrane at each temperature. Buffer only in the acceptor chamber (white bars); I-FABP in the acceptor chamber (gray bars). (C) Arrhenius plot of the rate of permeation (ln P_e) plotted as a function of the reciprocal of the absolute temperature in kelvins ($1/T$). (D) I-FABP facilitated membrane permeation model. C_mD and C_mA are the drug concentrations at the solution−membrane interface on donor and acceptor side boundary layers, respectively. C_D and C_A are the bulk concentration in the donor and acceptor compartments, respectively. C_{uwl}D and C_{uwl}A are the drug concentrations at the unstirred water layers on the donor and acceptor sides of the membrane. K_d and K_a are the partition coefficients for the interfacial partitioning between the donor solution and the membrane and between the acceptor solution and the membrane, respectively. dC_m/dt is the rate of membrane permeation. D is the diffusivity in the membrane. $h_{membrane}$ and h are the thickness of the membrane and hydrodynamic diffusion layers, respectively. The presence of an I-FABP protein sink significantly lowers K_a by promoting drug partitioning from the membrane into the acceptor chamber by internalizing the drug within its binding cavity, thereby lowering C_mA.

and is involved in the intracellular solubilization and transport of FA. In principle, this model for I-FABP-mediated transport is not limited to FA, but extends to any lipophilic molecule which selectively binds I-FABP. All lipophilic molecules will have inherently higher affinity for the membrane than the aqueous layer and therefore their diffusion will be limited by the same factors as FA: dissociation from the apical membrane and diffusion across the water layer. This study demonstrates that I-FABP is capable of binding specifically to a range of lipophilic drugs and facilitating their desorption from phospholipid membranes. Therefore, given the high levels of I-FABP protein expressed in the absorptive cells of the small intestine, it is likely that I-FABP also acts as a transporter for these molecules *in vivo*. Our model purports that I-FABP may enhance the rate of intracellular lipophilic drug desorption from the apical membrane of the enterocyte through binding and codiffusion of the drug molecule. In support of this theorem, we have utilized parallel artificial membranes with I-FABP protein sinks as a model of the intestinal epithelium in order to examine the kinetics and thermodynamics of lipophilic drug transport at the level of the biophysical barriers of the enerocyte. This model is

Table 3. Disappearance/Appearance Kinetics Permeability Values for Tolfenamic Acid Measured at pH 7.4 by the PAMPA Method

	P_e[a] (10^{-6} cm s^{-1})			
temp (°C)	**disappearance** buffer acceptor	**disappearance** I-FABP acceptor	**appearance** buffer acceptor	**appearance** I-FABP acceptor
15	1197 ± 236	937 ± 176	4.5 ± 1.8	9.8 ± 3.5
20	949 ± 147	611 ± 166	7.7 ± 1.7	13 ± 2.7
25	692 ± 106	550 ± 98	13 ± 4.6	20 ± 5.3
28	407 ± 79	352 ± 93	18 ± 3.4	28 ± 4.0
33	nd[b]	nd	34.2 ± 5.8	37 ± 5.1
37	nd	nd	37.5 ± 5.3	40 ± 6.5

[a] Mean ± sd, $n = 3$. [b] Not determined as data could not be fitted to equation model.[4]

supported by immunohistochemical studies of the small intestine that have shown that I-FABP is predominately localized to the enterocytic apical membrane forming the microvilli.[12,13] Localization of I-FABP to the membrane would allow for more efficient ligand uptake and release from the membrane by permitting ligand exchange without its entry into the aqueous phase. Coincidently, lipophilic drug absorption is believed to occur predominately at the tips of the micro-villus of the enterocytic apical membrane.[28]

If we consider the results from the artificial membrane model in thermodynamic terms, the effect of I-FABP was to significantly lower the activation energy for permeation of the test lipophilic drug, tolfenamic acid. This was also reflected as an increased desorption of the drug from the phospholipid membrane. The extent to which I-FABP lowers the activation energy for tolfenamic acid permeation across a membrane barrier (~5.4 kcal/mol) is more than surmounted by the net free energy of binding of tolfenamic acid to I-FABP in water ($\Delta G = -7.2$ kcal/mol). Figure 5D shows a schematic diagram of the artificial membrane permeability model that depicts the individual processes that mediate membrane permeation. Interpretation of the data in terms of this model suggests that the presence of I-FABP in the acceptor chamber solution significantly enhances the rate of permeation (dC_m/dt) across the membrane barrier. This effect is a product of the lower acceptor partition coefficient (K_a) due to the ability of I-FABP to decrease the drug concentration at the solution-membrane interface on the acceptor side (C_mA) by internalizing the drug within its binding cavity.

Energetic Coupling between Drug Binding and I-FABP Stability. In this study the global stability profiles of drug−I-FABP complexes were examined using the pulse proteolysis denaturant unfolding technique. The global stability of a protein depends on its Gibbs free energy of unfolding (ΔG_{unf}). At equilibrium where the folded and unfolded states are equal ($\Delta G_{unf} = 0$), this point corresponds to the midpoint of denaturation (~C_m). When a ligand binds specifically to the folded state, the free energy contribution from the binding interactions confers an increase in ΔG_{unf}, which results in a stabilizing effect observed as an increase in C_m. Therefore, the ligand dependent changes in the midpoint of denaturation result from the energetic coupling of ligand binding and protein unfolding. Drug binding to I-FABP is exothermic and is associated with improved bonding within the protein which decreases its internal motion thereby stabilizing the I-FABP structure as reflected in the higher C_m values.

Overall, our data signify that the structural tightening of the I-FABP fold from the reduced dynamics that accompany drug binding provides a large contribution of favorable binding energy toward drug complexation.

Thermodynamics of Drug Binding to I-FABP. The net free energy of drug binding to I-FABP is composed of energetic contributions from various interactions between drug, protein, and solvent. The composite enthalpic and entropic macroscopic terms are themselves composed of multiple synergistic and antagonistic microscopic components. Although a precise quantitative correlation of the individual microscopic components is not yet possible, a semiquantitative interpretation can be made based on available structural data as well as theoretical estimates from model systems. To better understand how drug−I-FABP interactions within the binding cavity are related to binding affinities we have attempted to interpret the thermodynamics data in terms of crystallographic and NMR chemical shift mapping models of each complex recently reported by our laboratory (Figure 6).[4]Although it is only semiquantitative, this nascent analysis is significant as it predicts the processes and interactions that drive the binding of lipophilic molecules to I-FABP, which is potentially an important factor in facilitating the desorption of lipophilic drugs from the apical enterocytic membrane. The changes in binding ($\Delta H°$) and order ($T\Delta S°$) are so complex that a useful approach is to express the net free energy of binding (ΔG) as the sum of free energies of individual opposing and synergistic energetic parameters (eq 7).[29,30] The average values from the energy parameters in eq 7 are based on correlations between crystallographic structural data with experimental thermodynamic binding data for a training set of small molecule ligands with their protein targets.[29,30] Supplementary Table 2 in the Supporting Information documents a comparison of measured and

(28) Camenisch, G.; Folkers, G.; van de Waterbeemd, H. Review of theoretical passive drug absorption models: Historical background, recent developments and limitations. *Pharm. Acta Helv.* **1996**, *5*, 309–327.

(29) Williams, D. H.; O'Brien, D. P.; Sandercock, A. M.; Stephens, E. Order changes within receptor systems upon ligand binding: receptor tightening/oligomerisation and the interpretation of binding parameters. *J. Mol. Biol.* **2004**, *340*, 373–83.

(30) Böhm, H. J. Prediction of binding constants of protein ligands: a fast method for the prioritization of hits obtained from de novo design or 3D database search programs. *J. Comput. Aided. Mol. Des.* **1998**, *12*, 309–323.

(31) Zídek, L.; Milos; Novotny, V.; Stone, M. J. Increased protein backbone conformational entropy upon hydrophobic ligand binding. *Nat. Struct. Biol.* **1999**, *12*, 1118–1121.

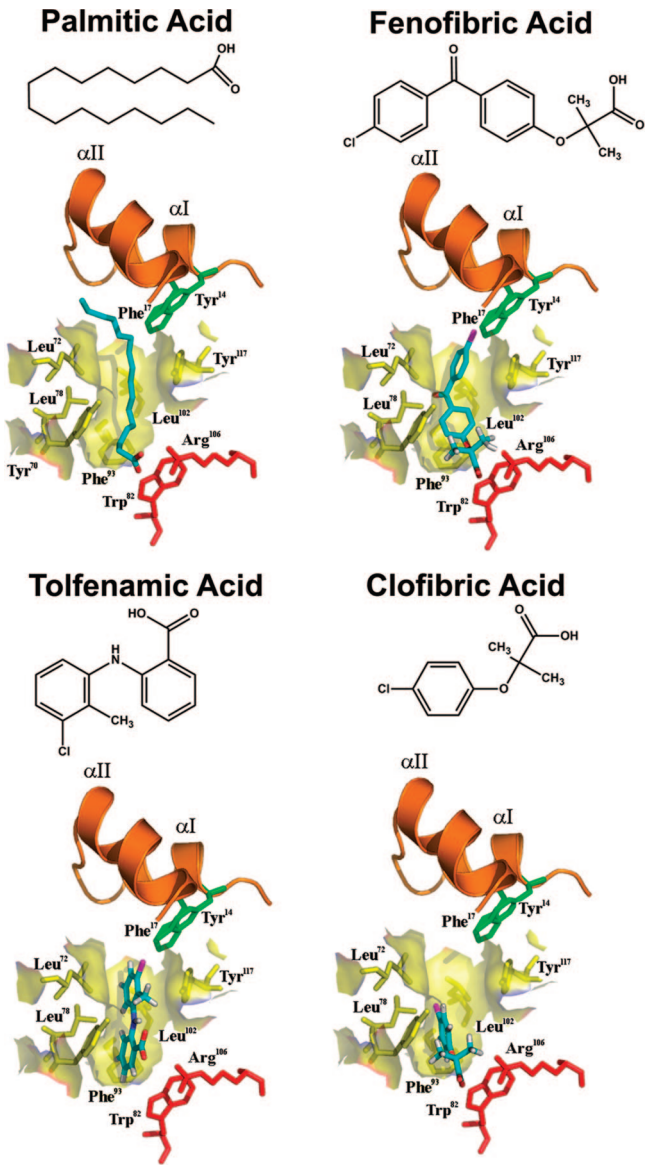

Figure 6. NMR [^{13}C-C$_\alpha$/C$_\beta$] chemical shift perturbation molecular docking models of each drug−I-FABP complex.[4] The side chains of cavity residues which form ionic and hydrogen bonds with the carboxylate moiety of each compound are shown in stick representation in red. The helical portal motif is shown in ribbon representation with the side chains of residues that contact the hydrophobic terminus of the ligand colored green. Residues forming the hydrophobic crevice that cradles the hydrophobic tail of each compound are shown in transparent surface and stick representation in yellow.

estimated thermodynamic parameters of drug binding which are discussed in more detail hereon in.

$$\Delta G = \Delta G_{\text{t+rProtein}} + \Delta G_{\text{t+rLigand}} + \Delta G_{\text{bw-I-FABP}} + \text{ÅÅ}\Delta G_{\text{h}} + \Delta G_{\text{hb}} + \Delta G_{\text{ionic}} + \Delta G_{\text{vdW}} \quad (7)$$

First, the enthalpic parameters of eq 7 will be discussed in detail. Enthalpic contributions to binding reflect protein−ligand interactions from hydrogen bonding, ionic interactions and van der Waals interactions relative to those existing with the solvent.

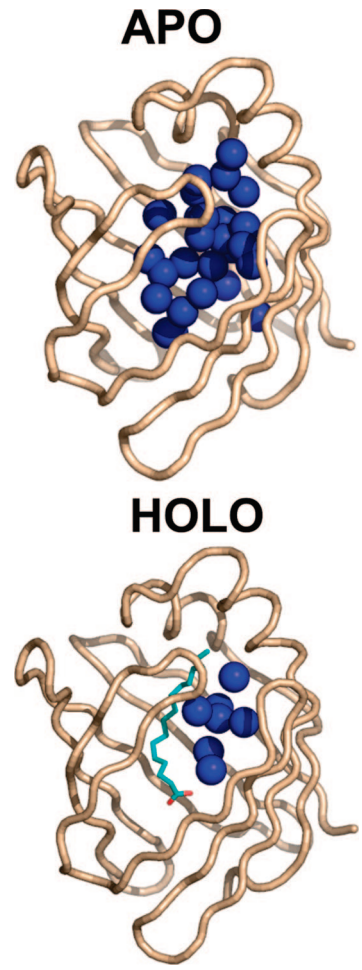

Figure 7. Ordered cavity water molecules shown in spheres are observed in the crystal structures of the apo- (1IFB) and holo-palmitate (2IFB) I-FABP crystal structures. The protein backbone is depicted in tube representation.

ΔG_{ionic} represents the free energy benefit from making an ionic bond of ideal geometry.[29,30] The large enthalpic contribution to the net free energy of binding of drugs that possess a terminal carboxylate is consistent with mutagenesis and crystallographic studies which show that ionic bonding interactions between the FA carboxylate and Arg^{106} is a key component of the binding process (Figure 6).[14]

ΔG_{vdW} is an enthalpic energy term that describes the contribution from van der Waals protein−ligand interactions. Crystal structures of I-FABP in complex with FA reveal numerous van der Waals interactions between the FA methylene tail and cavity side chains that provide important enthalpic contributions.[14] The methylene tail lies in a crevice lined with hydrophobic amino acids; this crevice also cradles the hydrophobic tail component of the drugs (Figure 6).

ΔG_{hb} represents the free energy benefit from making a hydrogen bond of ideal geometry. Co-crystal structures of

Table 4. Processes Related to the Thermodynamics of Lipophilic Drug Binding to I-FABP

Enthalpic Factors
Favorable
ionic and hydrogen bonding interaction between Arg^{106} and Trp^{82} with the drug carboxylate
van der Waals interactions between hydrophobic cavity side chains and the hydrophobic tail component of the drug
increased hydrogen bonding across the protein backbone from tightening of the structure upon drug binding
hydrogen bonding between remaining structural waters within the cavity and the drug
Opposing
the loss of hydrogen bonding between ordered cavity waters and cavity side chains upon desolvation of the cavity with ligand entry
Entropic Factors
Favorable
the hydrophobic effect from the burial of hydrocarbon surface from exposure to water and the loss of the hydration shell surrounding the hydrophobic drug molecule into the bulk solvent
expulsion of ordered water molecules from the binding cavity into the bulk solvent upon ligand binding
Opposing
loss of rotational and translational degrees of freedom in both the protein and ligand upon complexation
loss of degrees of freedom available to cavity waters when the ligand is bound

the FA−I-FABP complex show a hydrogen bond between the FA carboxylate and Trp^{82}.[14] Similarly, the NMR models show that the carboxylate of each drug is sufficiently proximal to Trp^{82} for hydrogen bonding (Figure 6). In addition ordered waters are observed around the bound FA, which would contribute a favorable enthalpy to the binding process through hydrogen bonding with the ligand.

The entropic parameters in eq 7 will be discussed hereon in. The entropy change from a ligand−protein binding event reflects primarily changes in solvation entropy and changes in conformational entropy in the protein and ligand.

The measured binding affinities of the lipophilic drugs examined were not directly related to their solubility or partition coefficients (Table 2), suggesting that the binding is driven by specific interactions between the drug and protein. $\text{Å}\Delta G_h$ represents the hydrophobic effect which is a favorable entropic contribution from the burial of hydrocarbon surfaces from exposure to water upon binding. The favorable entropy change from removal of hydrocarbon from exposure to water derives from the displacement of ordered water molecules at the hydrocarbon surface. In the case of the interaction of I-FABP with lipophilic drugs, the desolvation step is presumably driven by the hydrophobic effect which drives the drug out of the water phase and into the internalized cavity of I-FABP, thereby providing a favorable entropic contribution to the free energy of binding. Desolvation is a net entropic process; *in vivo* a lipophilic drug would preferentially partition into cellular membranes due to the favorable entropic forces of the hydrophobic effect. Subsequent partitioning from the membrane into the cavity of I-FABP is driven by the favorable net free energy of binding.

The term $\Delta G_{bw\text{-}I\text{-}FABP}$ is the free energy contribution due to displacement of ordered water from the binding cavity upon ligand binding. The binding cavity of I-FABP is occupied by solvent water molecules, many of which are ordered due to hydrogen bonding with cavity side chains or ordering of water around apolar residues (Figure 7).[14] A comparison of the crystallographic structures of the holo- and apo-protein clearly shows a loss of 20−25 water molecules from the cavity to accommodate the FA (Figure 7).[14] Provided that the cavity waters are more ordered than in bulk solution, one might expect a favorable entropic contribution to the binding free energy. This component consists of favorable entropic component resulting from the transfer of ordered water into the bulk solvent and an unfavorable ethalpic cost due to the disruption of hydrogen bonds between the ordered water molecules and cavity side chains.

Upon binding both the protein and the ligand lose some translational (t) and rotational (r) motion, which comes at an entropic cost (ΔG_{t+r}). The loss of ligand rotational and translational entropy ($\Delta G_{t+rLigand}$) has been estimated to be approximately 0.3 kcal/mol per internal rotor[29,30] (Supplementary Table 2 in the Supporting Information). Although comparisons of the apo- versus holo-I-FABP crystallographic structures show only minimal differences, comparison of the NMR solution state structures show significant differences in the helix II segment of the portal motif, which is disordered in the apo-protein.[15] The NMR chemical shift mapping data (Figure 3) indicate structural changes in I-FABP upon drug binding are predominately localized to the portal region, and when correlated with molecular models of each drug−I-FABP complex, the extent of conformational stabilization appears to be dependent on the ability of the hydrophobic tail component of a drug to participate in capping interactions with portal residues. This conformational stabilization was also shown to be coincident with the exchange rate of the drug−I-FABP complex, such that ligands in slow exchange (palmitic acid and fenofibric acid) formed longer lived complexes and thereby imparted a greater stabilizing effect. Quantification of the conformational entropy changes associated with the decrease in protein flexibility upon ligand binding is more complex given the large number of rotational and translational bonds within a protein's tertiary structure. NMR relaxation measurements have been developed for estimation of conformational entropy changes in a protein's backbone associated with ligand binding; however, the complexity of such an application is beyond the scope of this study. We have designated the as yet unidentified entropic penalty from the decrease in protein conformational freedom, $\Delta G_{t+rProtein}$; this value is estimated to be in the order of 20 to 30 kcal/mol to balance $\Delta G_{EstimatedTotal}$ with $\Delta G_{Measured}$. This is a plausible estimate if compared to the strongly unfavorable contribution to the entropy of binding of about 10 to 20 kcal/mol from

$\Delta G_{t+rProtein}$ in the case of the binding of 2-methoxy-3-isobutylpyrazine to mouse major urinary protein-I which displays a similar β-barrel fold as I-FABP and is also a member of the lipocalin superfamily.[31]

At first glance, the thermodynamics of lipophilic drug binding to I-FABP appears to be universally enthalpically driven. This is counterintuitive based on the expected favorable entropy gain from the hydrophobic effect of the burial of a hydrophobic ligand into the internalized protein cavity, together with the release of cavity waters into the bulk solvent. Nevertheless, the overall entropic contribution to the net free energy of binding for each drug is fairly modest. Presumably, the net entropy of binding amounts to almost zero due to balancing of a number of large, opposing entropic contributions. Thus, entropy still plays an important role in determining binding affinities due to the large and canceling composite entropic forces that give rise to the net entropy. It is likely the large favorable entropy from the hydrophobic effect and displacement of ordered cavity waters is canceled by the decrease in conformational entropy of the ligand and protein upon complexation. Therefore, it is more likely that the net free energy for binding of lipophilic drugs to I-FABP is an enthalpy−entropy driven process. Table 4 provides a summary of the individual enthalpic and entropic forces that favor or oppose lipophilic drug binding to I-FABP.

Conclusions/Significance

The broad application for this study is that poor understanding of the process by which lipophilic drugs are transported across the hydrophilic environment of the cytoplasm of enterocytes limits the effective design of drug candidates with optimal absorption characteristics. Over the past number of years considerable efforts have been directed toward rational drug design programs based on appreciation of drug binding to target receptors. However, progress in terms of identification of the structural determinants of compounds with favorable absorption, distribution, metabolism and elimination (ADME) characteristics (structure−transport relationships) has been far less evident. This study is timely and its significance heightened by the current trend within the pharmaceutical industry to utilize receptor-based screening techniques and combinatorial chemistry programs in pursuit of more active molecules: a situation which has resulted in the production of greater numbers of increasingly lipophilic and poorly absorbed drugs. An understanding of the mechanisms that mediate the transport of lipophilic drugs through the aqueous cytoplasm of the enterocyte is therefore a critical and currently limiting step in understanding the molecular determinants of drug leads that are orally available. It is likely that cytosolic transport proteins such as FABPs play a role in these processes. This study describes the thermodynamic properties of drug−I-FABP complexes, and also provides a preliminary indication of the importance of drug binding to I-FABP in the membrane desorption of lipophilic drugs. These data will provide a platform of information critical to the design of novel and biopharmaceutically advantageous drug molecules.

Acknowledgment. T.V. is the recipient of a Peter Doherty Fellowship (384300) from the National Health and Medical Research Council, Australia. This work was supported by grants from the Australian Research Council (DP0342458, DP0664069).

Supporting Information Available: Supplementary Figure 1 and Tables 1and 2. This material is available free of charge via the Internet at http://pubs.acs.org.

MP800227W